JOURNAL OF MATERIALS SCIENCE 29 (1994) 3705–3718

Thermally induced phase transformations of 12-tungstophosphoric acid 29-hydrate: synthesis and characterization of PW_8O_{26}-type bronzes

U. B. MIOČ
Faculty of Physical Chemistry, University of Belgrade, P.O.Box 137, 11001 Belgrade, Yugoslavia

R. Ž. DIMITRIJEVIĆ
Faculty of Mining and Geology, Department of Crystallography, University of Belgrade, Djusina 7, 11000 Belgrade, Yugoslavia

M. DAVIDOVIĆ
The Institute of Nuclear Sciences "Vinča", P.O.Box. 522, 11001 Belgrade, Yugoslavia

Z. P. NEDIĆ
Faculty of Physical Chemistry, University of Belgrade, P.O.Box 137, 11001 Belgrade, Yugoslavia

M. M. MITROVIĆ
Faculty of Physics, University of Belgrade, P.O.Box. 550, 11001 Belgrade, Yugoslavia

PH. COLOMBAN*
Laboratoire de Spectrochimie Infrarouge et Raman, CNRS, 2 rue Henri Dunant, 94320 Thiais, France

The phase transformations of 12-tungstophosphoric $H_3PW_{12}O_{40}$–$29H_2O$ (29-WPA) acid in the temperature range from ambient temperature to 1150 °C were investigated and characterized by differential thermal analysis (DTA), thermogravimetric analysis (TGA), differential scanning calorimetry (DSC), X-ray powder diffraction (XRPD), scanning electron microscopy (SEM), infrared (i.r.) and Raman spectroscopies. From room temperature to 550 °C, 29-WPA passes through a dehydration process, which characterizes the formation of different crystallohydrates, in anhydrous form as well as "denuded" Keggin's anions, the D-phase ($PW_{12}O_{38}$). During these processes, Keggin's anions are not disturbed too much and they are preserved up to about 550 °C. The "D" phase is transformed by solid– solid recrystallization at about 600 °C in a new monophosphate bronze type compound PW_8O_{26}. Unit cell dimensions were calculated from XRPD data ($a_0 = 0.7515$ nm). With the temperature increasing up to 1150 °C, novel synthesized cubic bronze passed through three polymorphous phase transitions. According to a general formula for monophosphate tungsten bronzes $(WO_3)_{2m}(PO_4)_4$ all four polymorphs have $m = 16$.

1. Introduction

Heteropolyacids, with a general formula of $H_{3+x}AM_{12}O_{40}$–nH_2O ($x = 0$–1; A = P, Si, B, As, Ge; M=Mo, W; $n = 30$–6) are of special interest as new materials because of their high conductivities. Due to their exceptionally high proton conductivity [1, 2] of $(100–3) \times 10^{-3}$ S cm^{-1}, they belong to the group of the few protonic conductors that are superionic at room temperature. Among these we pay attention to the 12-tungstophosphoric 29-WPA acid.

The study of the transformation of 12-tungstophosphoric acid, $H_3PW_{12}O_{40}$–$29H_2O$ (29-WPA), with temperature is interesting since the degree of dehydration has a remarkable role on the protonic-species equilibrium, on the proton mobility and on the mechanism of the proton conductivity. It is known that 29-WPA easily loses water and it is transformed into lower n-hydrates ($n = 21$, 14 and 6) depending on the temperature and relative humidity [2, 3]. The process of dehydration causes a decrease in conductivity [4] and some structural changes have also been observed [5, 6].

In previous studies of antimonic acid [7], zirconium phosphate [8] and uranyl-phosphate hydrates [9, 10],

*Author to whom all correspondence should be sent.

0022–2461

it was shown that the dehydration process leads both to the modification of protonic species and of the host lattice, which is followed by the transfer of protons from water to the framework. Heteropolyacid hydrates [11, 12] show the existence of a few protonic species (OH^-, H_2O, H_3O^+, $H_5O_2^+$) in a temperature-dependent equilibrium. However, because of the very sensitive equilibrium between different crystallohydrates of the *n*-WPA, the literature data are not consistent, and, at a higher temperature, data for some hydrates phases are missing.

In this paper we report a study of the calcination/dehydration and structural modification of WPA hydrates from room temperature to 1150 °C. We also investigated the accompanying modifications of the protonic species during the dehydration process as well as the synthesis of phosphorus–tungsten bronzes and their polymorphous transformations.

2. Samples and techniques

29-WPA acid was synthesized according to the procedure described in detail in [11].

Differential scanning calorimetry (DSC) was performed using a DSC 4 Perkin Elmer and Netzsch simultaneous thermal Analysers STA 409 EP (scanning rate 1–10 K min^{-1}). Thermogravimetric analysis (TGA) and differential thermal analysis (DTA) were performed using a TGA Dupont Nemours instrument, as well as a Stanton-Rederoft 1000. The instruments were calibrated with potassium oxalate. Measurements of thermal transformations were made in an atmosphere of nitrogen, with a flow rate of 50 ml min^{-1}. Scanning rates were 1, 5 and 10 K min^{-1}.

X-ray powder diffraction (XRPD) patterns were obtained on a Phillips PW-1710 automated diffractometer, with a copper tube operated at 40 kV and 35 mA. The instrument was equipped with a diffracted beam curved graphite monochromator and an Xe-filled proportional counter. Diffraction data were collected in the 2θ range from 4° to 70°, counting for 2.5 s at each 0.02° 2θ step. A fixed 1° divergence and 0.1° receiving slits were used. A silicon powder was used as the standard for calibrating the diffractometer. All the XRPD experiments were performed at room temperature. Use was made of the trial-and-error indexing programs TREOR [13] and VISSER [14], of a program for the refinement of cell dimensions, LSUCRIPC [15], and of a version of an Appleman and Evans [16] program adapted for a personal computer.

Investigations of the crystal morphology were carried out with a scanning electron microscopy (SEM JSM 840A Jeol).

The WPA samples for X-ray diffraction (XRD) and SEM analysis were prepared in the same manner. They were heated to different temperatures, with a heating rate of 1° min^{-1} for temperatures below 100 °C. For temperatures above 100 °C the heating rates were 5° min^{-1} and 10 °C min^{-1}. The samples were kept at a given temperature for 10 min. Exposure of the samples to the given temperatures for 1 h showed that there was no influence of the heating time on the stability of the crystalline phase.

Infrared (i.r.) spectra of sample mulls in Nujol and Fluorolube were recorded on Perkin-Elmer spectrophotometers, (types 983G and FT-IR 1720X).

Raman spectra of polycrystalline samples sealed in glass tubes were examined on a Dilor RII instrument, using 488 and 514 nm exciting lines from a Spectra Physics laser. Raman spectra were also made with a Raman microsonde Microdil 28 Dilor. Always starting from single crystals with 29 molecules of water, except when the nature of experiment required otherwise, the laser power was systematically changed by one laser wavelength (mostly for $\lambda = 487.987$ nm, and more rarely for $\lambda = 514.53$ nm). An increase in the laser power corresponded to an increase in the temperature, which allowed us to follow the spectral change as a function of the laser power, that is, temperature.

The content of phosphorus, especially in the bronzes, was controlled by XRF spectrophotometer ORTEC-TEFA model 6111 with an Si–(Li) detector. The K_α line (2.01 eV) of phosphorus was used.

The chemical analyses of phosphorous bronze synthesized over 600 °C were made gravimetrically.

3. Results and discussion

3.1. Water loss and influence on the Keggin's ion framework

The results of the thermal analysis of 29-WPA from room temperature to 1150 °C are presented in Fig. 1. Three events were observed: a doublet at 50 °C (endothermic) and two peaks at about 170 °C (endothermic) and 600 °C (exothermic). Two other features must be noted: a glass-transition temperature, T_g, anomaly at about 400 °C and a large noise above 700 °C. The first doublet can be resolved into two components at about 30° and 40 °C; this corresponds to the formation of 21-WPA and 14-WPA hydrates, Fig. 1a.

The phase transformation of the 14-WPA to the 6-WPA hydrate is a fast process. The formation of the 6-WPA phase finished at about 60 °C and it remained stable up to 170 °C, Fig. 1a. Above this temperature another endothermic transformation was evident. The sample loses, in two steps, between 170 and 240 °C, 5.8–6.0 molecules of water, Fig. 1b. In consideration of the sensitivity of the sample to the partial pressure of water and to the experimental conditions, it could be concluded that six molecules of water are lost and an anhydrous phase of WPA (0-WPA) is formed. This means that there would be no more crystalline water present, only the free protons ($H_3PW_{12}O_{40}$). The 0-WPA phase is stable up to about 410 °C, Fig. 1b.

On the DTA curve, the T_g anomaly at about 400 °C (broad peak) is evident. It corresponds to the exothermic transformation, which is followed by the loss of mass corresponding to one water molecule, Fig. 1b. This confirms the assumption that, in the 0-WPA phase, only acid protons are present. This water molecule is formed from protons and oxygen from the host lattice. The exothermic process of water forma-

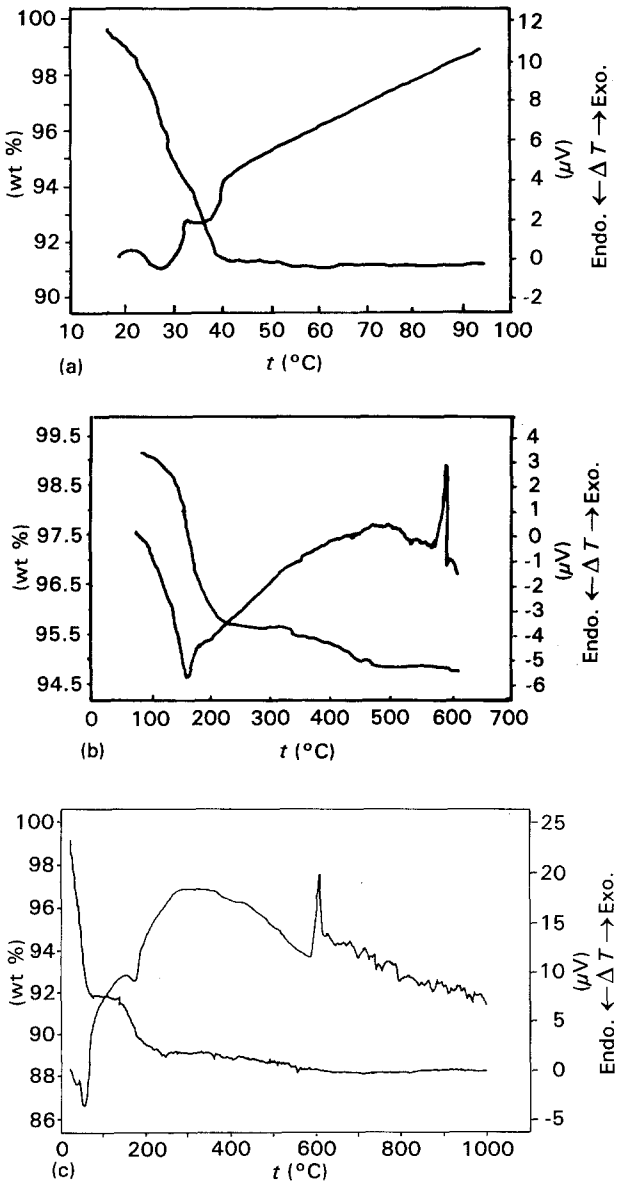

Figure 1 DTA and TGA curves of 29-WPA at temperatures up to 1000 °C (10 °C min^{-1}): (a) details at (about) 40 °C (1 °C min^{-1}), and (b) details in the range 100–500 °C (5 °C min^{-1}).

tion and the endothermic process of dehydration are simultaneous, so that the peak is broad. This process is finished at about 440 °C, when denuded Keggin's anions, the D-WPA phase, formed. All these processes are very complex. To resolve them completely new studies are necessary. Some kinetic measurements are in progress [17].

Fournier *et al.* [18] noted the same large peak for WPA and identified a new Q-phase in the atmosphere of oxygen at 350 °C. According to their results, this Q-phase is formed after the loss of "constitutional" water. In contrast to their results, up to 350 °C we found only protons. The Q-phase can only be a mixture of two phases, 0-WPA and D-WPA.

The exothermic DTA peak at 602 °C corresponds to a recrystallization of Keggin's anions and to bronze formation; this will be discussed later.

The XRPD and SEM investigations of the WPA transformations in the temperature range 20–1150 °C were carried out on the samples chosen with reference to the results of the thermal measurements presented in Fig. 1.

In the temperature range 20–60 °C, during the process of dehydration, the starting heteropolyacid 29-WPA underwent two symmetry transformations before the stable 6-WPA phase was formed. The XRPD patterns of the WPA phases with 29, 21, 14 and 6 molecules of water are presented in Fig. 2. The measured and indexed powder patterns are listed in Tables I and II. The corresponding unit-cell dimensions are presented in Table III. The results obtained for the 29-WPA and 21-WPA phases are in excellent agreement with the data given in [19–21]. However, close examinations of the XRPD patterns of these phases revealed several weak superstructure lines, which possibly point to a higher symmetry and ordering in the crystal structures. The powder pattern of the 14-WPA phase, obtained from the dehydration process of the 21-WPA at 38 °C, was indexed in triclinic symmetry by analogy with the

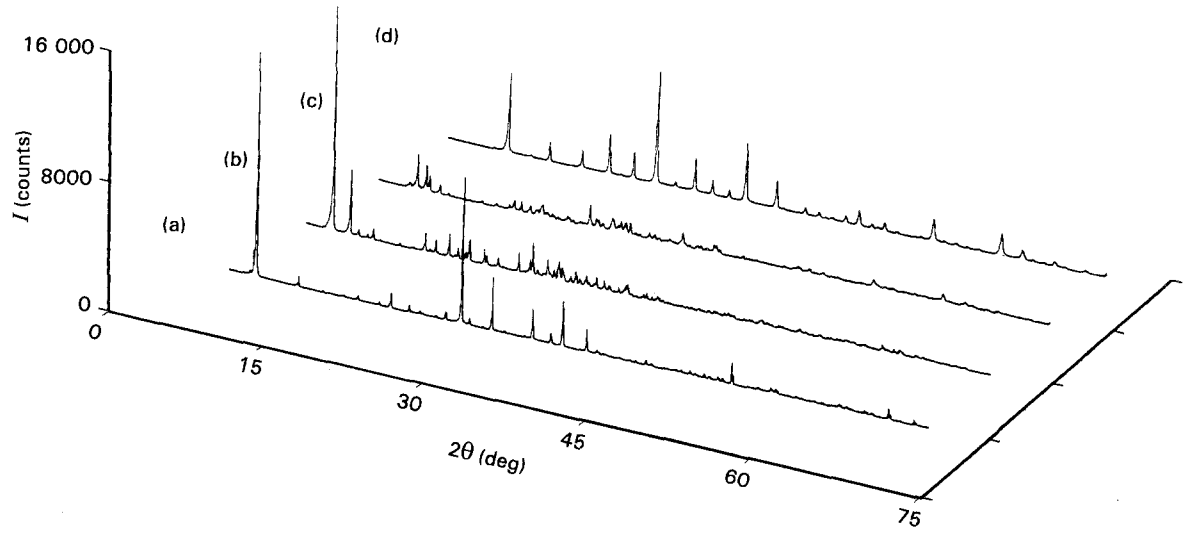

Figure 2 XRPD traces of different WPA heteropolyacid phases: (a) 29-WPA acid at 22 °C, (b) 21-WPA acid at 28 °C, (c) 14-WPA acid at 43 °C, and (d) 6-WPA acid at 60 °C.

TABLE I The XRPD data for 29-WPA (room temperature) and for 21-WPA (calcined at 28 °C)

29-WPA						21-WPA											
I/I_0	H	K	L	D_c (nm)	D_0 (nm)	I/I_0	H	K	L	D_c (nm)	D_0 (nm)	I/I_0	H	K	L	D_c (nm)	D_0 (nm)
100	1	1	1	1.34685	1.33515	100	0	1	0	1.30972	1.30560	1	8	2	0	0.24190	0.24166
4	2	2	0	0.82477	0.82143	29	2	0	0	1.04127	1.04127	3	3	3	6	0.23993	0.23976
1	2	2	2	0.67342	0.67172	3	0	0	2	0.94633	0.94533	2	0	0	8	0.23658	0.23657
1	4	0	0	0.58320	0.58249	2	1	0	2	0.86155	0.86089	1	5	2	6	0.23475	0.23491
3	3	3	1	0.53518	0.53434	5	2	1	0	0.81506	0.81464	3	3	4	5	0.23324	0.23318
1	4	2	2	0.47618	0.47576	1	0	1	2	0.76706	0.76679	1	7	1	5	0.23026	0.23031
13	5	1	1	0.44895	0.44838	1	1	1	2	0.71978	0.71986	1	2	1	8	0.22721	0.22738
5	4	4	0	0.41239	0.41197	1	0	2	0	0.65486	0.65490	1	5	1	7	0.22346	0.22337
2	5	3	1	0.39432	0.39385	1	1	2	1	0.59322	0.59355	1	2	4	6	0.22195	0.22185
1	4	4	2	0.38880	0.38892	8	2	2	0	0.55434	0.55425	1	5	5	1	0.22023	0.22019
1	6	2	0	0.36885	0.36843	2	0	2	2	0.53850	0.53902	1	5	3	6	0.21790	0.21797
5	5	3	3	0.35575	0.35554	1	2	2	1	0.53200	0.53227	1	8	2	4	0.21539	0.21551
95	4	4	4	0.33671	0.33640	6	1	2	2	0.52135	0.52063	1	1	5	5	0.21426	0.21414
1	7	1	1	0.32666	0.32672	1	3	1	2	0.51470	0.51493	1	2	6	1	0.21229	0.21234
1	6	4	2	0.31173	0.31149	1	2	1	3	0.49890	0.49953	1	4	3	7	0.21028	0.21034
9	7	3	1	0.30371	0.30351	10	4	1	0	0.48381	0.48399	1	6	5	1	0.20782	0.20781
2	8	0	0	0.29160	0.29150	1	2	2	2	0.47832	0.47843	2	9	1	4	0.20530	0.20527
1	7	3	3	0.28450	0.28471	1	4	1	1	0.46874	0.46902	1	6	5	2	0.20416	0.20409
1	8	2	2	0.27492	0.27486	5	3	2	1	0.46194	0.46154		2	3	8	0.20397	
24	7	5	1	0.26937	0.26931	4	0	1	4	0.44502	0.44416	1	8	4	1	0.20260	0.20261
1	8	4	0	0.26082	0.26068	3	3	1	3	0.43977	0.44013	2	5	3	7	0.20125	0.20114
2	9	1	1	0.25606	0.25602	10	0	3	0	0.43658	0.43596		10	1	2	0.20098	
7	6	6	4	0.24868	0.24861	1	2	2	3	0.41643	0.41616	2	5	4	6	0.19944	0.19948
3	7	7	1	0.23446	0.23446	7	4	2	0	0.40753	0.40749	1	9	2	4	0.19813	0.19806
1	10	2	0	0.22875	0.22873	4	2	3	0	0.40262	0.40275	1	1	6	4R[a]	0.19732	0.19712
1	9	5	1	0.22552	0.22555	1	3	0	4	0.39098	0.39094		4	6	2R[a]	0.19690	
1	10	2	2	0.22447	0.22428	4	4	1	3	0.38392	0.38411	1	6	1	8	0.19335	0.19333
1	9	5	3	0.21754	0.21752		0	2	4	0.38352		1	6	5	4	0.19124	0.19117
1	10	4	2	0.21296	0.21299	1	1	2	4	0.37718	0.37721	1	7	4	5	0.19033	0.19034
1	11	1	1	0.21034	0.21036	1	4	2	2	0.37430	0.37455	2	7	5	3	0.18770	0.18775
4	8	8	0	0.20619	0.20625		3	1	4	0.37464		2	4	2	9	0.18688	0.18683
1	11	3	1	0.20382	0.20387	1	2	3	2	0.37048	0.37047	2	2	3	9	0.18640	0.18630
1	10	6	0	0.20004	0.20007	8	1	3	3	0.35378	0.35394		2	0	10	0.18622	
1	12	0	0	0.19440	0.19443	1	6	0	0	0.34709	0.34716	1	1	7	1	0.18546	0.18549
2	11	5	1	0.19241	0.19243	1	4	2	3	0.34232	0.34237	1	5	6	3	0.18486	0.18496
2	12	2	2	0.18922	0.18924	6	2	3	3	0.33939	0.33968	1	8	5	1	0.18377	0.18371
1	11	5	3	0.18738	0.18740	14	6	1	0	0.33551	0.33597	1	3	1	10	0.18085	0.18087
1	12	4	0	0.18442	0.18446		3	2	4	0.33570		1	10	3	3	0.18014	0.18016
3	9	9	1	0.18272	0.18275	2	5	2	2	0.32946	0.32992	2	8	0	8	0.17508	0.17509
1	10	8	2	0.17998	0.17998	1	0	4	0	0.32743	0.32766	1	10	3	4	0.17468	0.17461
1	13	1	1	0.17840	0.17844	1	1	2	5	0.32374	0.32387		7	5	5R[a]	0.17447	
2	12	4	4	0.17584	0.17584	7	3	3	3	0.31888	0.31904	1	7	6	2	0.17303	0.17300
1	13	3	1	0.17436	0.17453		1	4	1	0.31883			11	3	1	0.17296	
1	13	3	3	0.17060	0.17061	2	4	3	2R[a]	0.31540	0.31589	1	2	3	10	0.17128	0.17124
3	8	8	8	0.16834	0.16838	4	2	4	0	0.31235	0.31216		8	4	6	0.17116	
1	13	5	1	0.16706	0.16709		1	0	6	0.31189		1	9	4	5R[a]	0.16907	0.16892
7	14	2	0	0.16495	0.16500	5	2	4	1	0.30818	0.30851	1	7	5	6	0.16685	0.16689
3	13	5	3	0.16373	0.16376		4	2	4	0.30879		1	8	6	2	0.16471	0.16471
2	14	2	2	0.16333	0.16333	8	6	2	0	0.30668	0.30709		10	4	4	0.16473	
1	11	9	3	0.16060	0.16061		5	2	3	0.30702			6	7	0	0.16470	
1	14	4	0	0.16022	0.16020		0	1	6	0.30667		1	0	8	0	0.16372	0.16376
1	14	4	2	0.15873	0.15874	5	5	1	4	0.30409	0.30424	1	1	8	1	0.16261	0.16268
1	13	7	1	0.15764	0.15765	4	6	2	1	0.30273	0.30303	1	9	4	6R[a]	0.16211	0.16198
1	12	8	4	0.15587	0.15592		1	1	6	0.30340		1	1	7	6	0.16044	0.16044
1	15	1	1	0.15483	0.15483	3	6	1	3	0.29622	0.29622	1	2	8	2	0.15942	0.15940
1	14	6	0	0.15316	0.15318		3	2	5	0.29634			10	4	5	0.15939	
1	15	3	1	0.15218	0.15219	6	3	3	4	0.29125	0.29118	1	9	6	1	0.15823	0.15822
1	14	6	2	0.15185	0.15182	2	1	4	3	0.28783	0.28779		12	2	4R[a]	0.15811	
4	15	3	3	0.14965	0.14965	4	5	2	4	0.28213	0.28212	1	8	6	4	0.15770	0.15771
2	12	10	2	0.14813	0.14812	2	2	4	3	0.27992	0.27976	3	4	8	2	0.15409	0.15404
1	15	5	1	0.14725	0.14723	1	4	4	0	0.27717	0.27706		9	6	3	0.15398	
1	15	5	3	0.14495	0.14494		7	1	2	0.27737		2	7	6	6	0.15369	0.15365
						2	6	2	3	0.27582	0.27577		7	7	3	0.15362	
							2	3	5	0.27578		1	2	8	4	0.15304	0.15304
						5	5	1	5	0.27393	0.27388		8	6	5	0.15299	
							6	1	4	0.27369		2	4	8	3R[a]	0.15160	0.15150
						3	7	2	1	0.26813	0.26806		11	5	2	0.15146	
							3	4	3	0.26808		2	9	6	4	0.15053	0.15047
						2	3	3	5	0.26443	0.26441		5	8	2	0.15043	
						2	7	1	3	0.26358	0.26350	1	2	8	5	0.14872	0.14866
						1	8	0	0	0.26032	0.26031	1	14	0	2	0.14695	0.14697
						2	5	2	5	0.25755	0.25745	1	12	4	4	0.14587	0.14588
							1	5	1	0.25748			11	5	4	0.14596	
						1	8	1	0	0.25532	0.25521	1	9	7	2	0.14380	0.14375
							5	4	1	0.25506		1	14	1	4	0.14108	0.14106
						2	5	3	4	0.25418	0.25406		12	5	3	0.14101	
						4	8	1	1	0.25303	0.25295	1	4	8	6	0.13996	0.13990
						5	7	0	4	0.25186	0.25171		7	8	3	0.13986	
							2	5	1	0.25177		1	8	8	0R[a]	0.13859	0.13851
						1	7	2	3	0.24889	0.24877	1	15	1	2	0.13662	0.13657
						1	1	4	5	0.24591	0.24588	1	1	9	5	0.13554	0.13555

[a]R-rejected line

TABLE II The XRPD data for WPA (calcined at 42 °C) and for 6-WPA (calcined at 170 °C)

14-WPA												6-WPA					
I/I_0	H	K	L	D_c (nm)	D_0 (nm)	I/I_0	H	K	L	D_c (nm)	D_0 (nm)	I/I_0	H	K	L	D_c (nm)	D_0 (nm)
17	0	0	1	1.23291	1.22772	8	−5	−5	2	0.24271	0.24242	66	1	1	0	0.85927	0.85797
100	1	1	0	1.10768	1.10099		−1	3	3	0.24236		2	1	1	1	0.70159	0.70084
7	−1	−1	1	1.07226	1.06460	22	−3	3	0	0.23800	0.23832	16	2	0	0	0.60760	0.60732
72	0	−1	1	0.99424	0.99467	20	5	3	1	0.23673	0.23657	15	2	1	1	0.49610	0.49607
46	−1	0	1	0.95815	0.95604		−4	1	3	0.23648		36	2	2	0	0.42964	0.42970
9	1	0	1	0.79107	0.79316	11	−6	−3	2	0.23455	0.23476	1	2	2	1	0.40506	0.40519
3	0	1	1	0.76490	0.76316	1	−1	4	2	0.22862	0.22834	24	3	1	0	0.38428	0.38428
1	2	1	0	0.65952	0.66197		−2	−6	1	0.22815		100	2	2	2	0.35080	0.35079
8	2	2	0	0.55384	0.55168	3	−6	−2	3R[a]	0.22435	0.22476	4	3	2	1	0.32477	0.32485
1	−2	−2	2	0.53613	0.53482	9	1	1	5	0.22207	0.22192	29	4	0	0	0.30380	0.30389
11	2	1	1	0.51202	0.51242	3	2	5	2	0.21462	0.21463	13	3	3	0	0.28642	0.28640
3	0	2	1	0.48996	0.48888	2	−6	−1	3	0.21202	0.21187	7	4	2	0	0.27173	0.27174
27	−2	0	2	0.47908	0.47881		5	0	2	0.21167		51	3	3	2	0.25908	0.25900
1	−2	1	0	0.46666	0.46756	1	−3	1	5	0.20865	0.20847	1	4	2	2R[a]	0.24805	0.24758
6	−3	−1	1	0.46124	0.46225		2	1	5	0.20836		23	5	1	0	0.23832	0.23829
21	−3	−2	1R[a]	0.45934	0.45660	7	−7	−3	3	0.19871	0.19861	1	5	1	1	0.23386	0.23382
	1	−2	1R[a]	0.45375		13	−7	−3	1	0.19719	0.19720	5	5	2	1	0.22186	0.22185
14	−2	1	1	0.44324	0.44416		6	4	1	0.19707		4	4	4	0	0.21482	0.21485
16	3	1	0	0.44046	0.44045	9	−3	−7	1	0.19608	0.19614	1	4	4	1R[a]	0.21154	0.21128
29	−1	−3	2	0.43360	0.43312	6	−7	−2	1	0.19402	0.19402	2	5	3	0	0.20840	0.20847
12	0	−1	3	0.42345	0.42402	10	−4	1	5	0.19220	0.19216	6	6	0	0	0.20253	0.20253
14	−2	−1	3	0.42080	0.42035	10	6	3	2	0.18742	0.18744	13	6	1	1	0.19713	0.19714
12	0	0	3	0.41097	0.41084	3	4	−3	3	0.18255	0.18259	4	6	2	0	0.19214	0.19206
6	3	0	0R[a]	0.40253	0.40059	3	2	7	1	0.17474	0.17464	2	5	4	0	0.18978	0.18979
5	0	−2	3	0.38813	0.38842		3	3	5	0.17453		7	5	4	1	0.18751	0.18751
11	1	2	2	0.38112	0.38111	21	6	−1	2	0.17197	0.17185	2	6	2	2	0.18320	0.18325
7	−2	0	3	0.37430	0.37493		1	5	4	0.17175		1	4	4	4	0.17540	0.17531
5	2	−1	2	0.36410	0.36376	6	6	0	3	0.16858	0.16853	20	7	1	0	0.17185	0.17190
3	0	1	3	0.36109	0.36086		−8	−2	3	0.16843		2	6	4	0	0.16852	0.16853
24	1	1	3	0.34209	0.34211	6	−8	−6	2R[a]	0.16658	0.16633	2	7	2	1	0.16537	0.16536
20	−4	−1	1	0.33956	0.33929	5	7	1	2R[a]	0.16400	0.16373	1	6	4	2	0.16239	0.16232
	−2	2	1	0.33917			3	8	0	0.16357		1	7	3	0	0.15956	0.15953
14	−4	−3	1R	0.33315	0.33399	5	−6	−8	1	0.16122	0.16111	18	6	5	1	0.15433	0.15434
	−1	−4	2	0.33396		3	7	7	0	0.15824	0.15819	8	8	1	1	0.14958	0.14958
31	3	−1	1	0.32164	0.32130		6	1	4	0.15816		2	8	2	0	0.14736	0.14737
19	3	1	2	0.31608	0.31576	21	−1	7	1	0.15436	0.15434	1	6	5	3	0.14524	0.14521
31	−1	3	1	0.31345	0.31294		4	8	1	0.15420		5	6	6	0	0.14321	0.14328
28	3	4	0	0.30812	0.30875	11	−2	−9	2	0.14963	0.14950	1	7	5	0	0.14126	0.14124
31	0	0	4	0.30823	0.30807		1	8	1	0.14946		2	7	5	2	0.13759	0.13763
22	−1	−3	4	0.30698	0.30698	6	4	7	3	0.14802	0.14794						
	−3	−3	4	0.30681			−9	−2	1	0.14791							
	−4	0	1	0.30697		4	8	1	2	0.14524	0.14518						
8	−4	−4	1	0.29767	0.29772	7	8	5	2	0.14328	0.14325						
6	−4	0	2	0.29401	0.29394	2	4	−6	1	0.14198	0.14191						
15	−4	−3	4	0.28076	0.28100		−6	4	0	0.14187							
8	−3	2	1	0.27720	0.27689	1	9	2	1	0.13910	0.13907						
11	−4	−4	4	0.26807	0.26845		−2	7	2	0.13909							
4	−5	−1	2	0.26380	0.26384		7	8	1	0.13909							
	3	0	3	0.26369			−3	6	3	0.13909							
9	−3	−2	5	0.26095	0.26086		−4	6	1	0.13900							
5	0	−1	5R[a]	0.25478	0.25406	3	6	7	3	0.13755	0.13759						
8	−1	4	1R[a]	0.24986	0.24921	2	−7	3	2	0.13720	0.13723						
	0	−4	4R[a]	0.24856		1	6	6	4R[a]	0.13565	0.13578						
10	0	−5	1	0.24635	0.24659												

R- rejected line

$H_3PMO_{12}O_{40}$–$13H_2O$ [22] and $NaH_2PW_{12}O_{40}$ –$14H_2O$ [23] phases.

The XRPD data also confirmed that the phase transformations of 14-WPA to 6-WPA is a very fast process: about 20% of the hexahydrate phase had already formed at 42 °C. The measured and indexed powder patterns and the corresponding cell dimensions of the hydrates are presented in Tables II and III. These measurements are in good agreement with the results obtained for single-crystal measurements presented in [18–22]. From the measurements of the unit-cell dimensions of the 6-WPA at different temperatures, Table III and Fig. 3, it could be concluded that this phase is stable up to 170 °C.

The SEM study of the 29-WPA dehydration showed that lower hydrates were obtained by a solid–solid

TABLE III The unit-cell dimensions of various WPA heteropoly acid phases and synthesized PW_8O_{26} bronze polymorphs at different calcination temperatures

Sample	Calcination temperature (°C)	a_0 (nm)	b_0 (nm)	c_0 (nm)	α_0 (degrees)	β_0 (degrees)	γ_0 (degrees)	V_0 (nm^3)
29-WPA	Room temperature	2.3328 (2)						12.695 (4)
21-WPA	28	2.0825 (2)	1.3097 (1)	1.89266 (4)				5.1623 (8)
14-WPA	42	1.4075 (4)	1.4121 (4)	1.3525 (3)	112.01 (2)	109.62 (2)	60.89 (1)	2.142 (1)
6-WPA	42	1.2149 (3)						1.793 (1)
6-WPA	80	1.2152 (1)						1.7945 (6)
6-WPA	Over P_2O_5	1.2151 (2)						1.7941 (7)
6-WPA	130	1.2144 (1)						1.7911 (6)
6-WPA	170	1.21513 (3)						1.7942 (3)
n-WPA ($n < 6$)	200	1.2086 (5)						1.765 (2)
n-WPA ($n < 6$)	220	1.2071 (4)						1.759 (2)
0-WPA	250	1.2166 (3)						1.801 (1)
0-WPA	300	1.2166 (4)						1.801 (2)
0-WPA	350	1.2185 (6)						1.809 (2)
0-WPA	400	1.2130 (4)						1.784 (2)
D-WPA	450	1.149 (1)						1.518 (5)
PW_8O_{26}	650	0.7515 (7)						0.424 (1)
PW_8O_{26}	750	0.7325 (6)	0.7516 (9)	0.7686 (9)		90.79 (5)		0.4231 (9)
PW_8O_{26}	1050	1.2321 (6)	2.3787 (9)	11.926 (2)				3.495 (4)
PW_8O_{26}	1150	0.7310 (1)	0.7524 (1)	0.7686 (1)	88.90 (1)	90.98 (1)	90.94 (1)	0.4225 (1)

The error (in brackets) is related to the last given number.

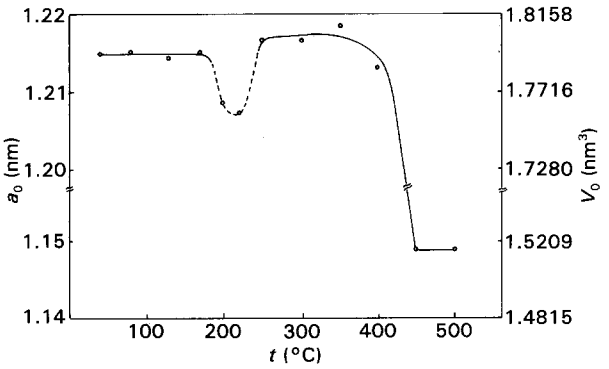

Figure 3 Changes of the unit cell dimensions of the 6-WPA phase in the temperature range 42–500 °C.

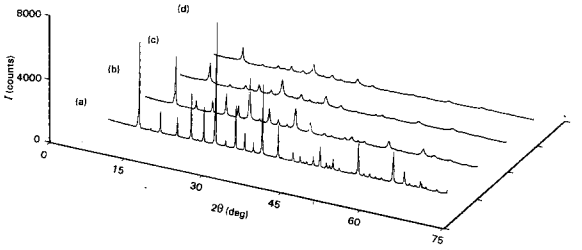

Figure 4 The XRPD traces of calcined 6-WPA phase at different temperatures: (a) 6-WPA at 170 °C, (b) 0-WPA at 250 °C (c) 0-WPA at 350 °C, and (d) 0-WPA at 400 °C.

recrystallization process. The SEM microphotographs of the sample heated at 60 °C (pure 6-WPA phase) show that fissures parallel to (1 0 0) are dominant (Fig. 6a). The crack process in WPA crystals followed the appearance of smaller crystals of the order 0.1 μm until the stable 6-WPA phase was formed. Heating above 60 °C led to solid–solid recrystallization, where larger, cubic, single-crystals appeared. Depending on the increase in temperature, different crystal forms and sizes were observed. Fig. 6b, shows that the 6-WPA crystals heated at 130 °C have rhombicdodecahedral and octahedral forms. At this temperature, interpenetrated twins were also observed.

Heating of the 6-WPA above 170 °C, Fig. 4a, leads to considerable structural changes and to a reduction in the intensities; see Fig. 4. In the temperature range 170–250 °C, Fig. 3 and Table III, a slight decrease in the unit-cell dimensions is evident, with a minimum between 200 °C and 220 °C, which is consistent with the dehydration at about 200 °C (from the DTA and DSC data). From structural aspects, these changes are certainly caused by dehydration of the 6-WPA phase; that is, the 0-WPA phase with the composition $H_3PW_{12}O_{40}$ is formed.

Continuation of calcination above 250 °C leads to a slight increase in the unit-cell dimensions, Fig. 3, of the 0-WPA phase and to a further reduction in the intensities and to a consequent increase of the background. These changes can be followed in the temperature range 250–400 °C, Fig. 4b–d, and Table III. The nature of the changes in the unit-cell dimensions could lie in the mutual electrostatic repulsion of Keggin's anions which results in an elongation of the hydrogen bonds between them. A relatively high background is possibly a consequence of the positional disorder of oxygen atoms.

From Figs 4d and 5a, it is evident that the 0-WPA phase is stable at 400 °C; that is Keggin's ion structure is preserved, Table V. The SEM investigation at 350 °C, Fig. 6c, confirmed that the cubic symmetry and crystal forms of the 0-WPA phase were preserved. An XRPD experiment on the 0-WPA sample at 350 °C and D-WPA at 500 °C in a wet atmosphere showed that the samples were completely reversible to the 6-WPA phase. This is consistent with the thermal measurements in [17].

Increasing the temperature in the range 400–450 °C led to a new phase transition. By solid–solid recrystallization the 0-WPA ($H_3PW_{12}O_{40}$) phase,

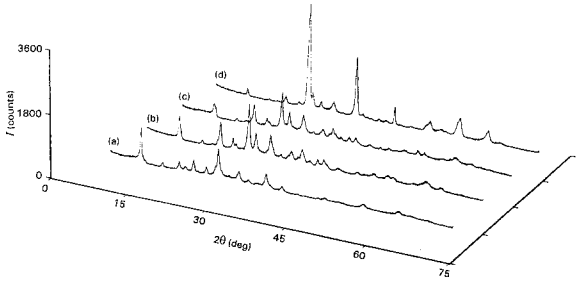

Figure 5 The XRPD traces of 0-WPA ($H_3PW_{12}O_{40}$) phase transformation at different temperatures: (a) 0-WPA at 400 °C, (b) D-WPA at 450 °C, (c) D-WPA at 500 °C, and (d) D-WPA and PW_8O_{26} bronze phases at 550 °C.

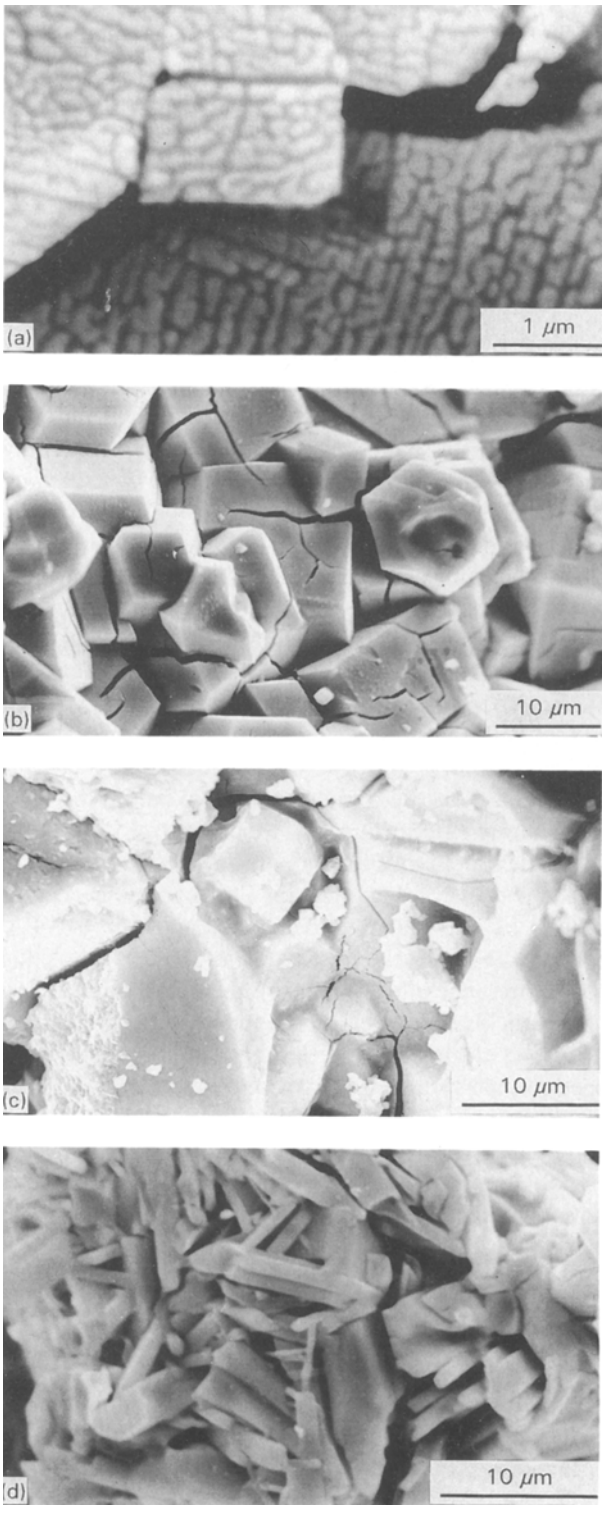

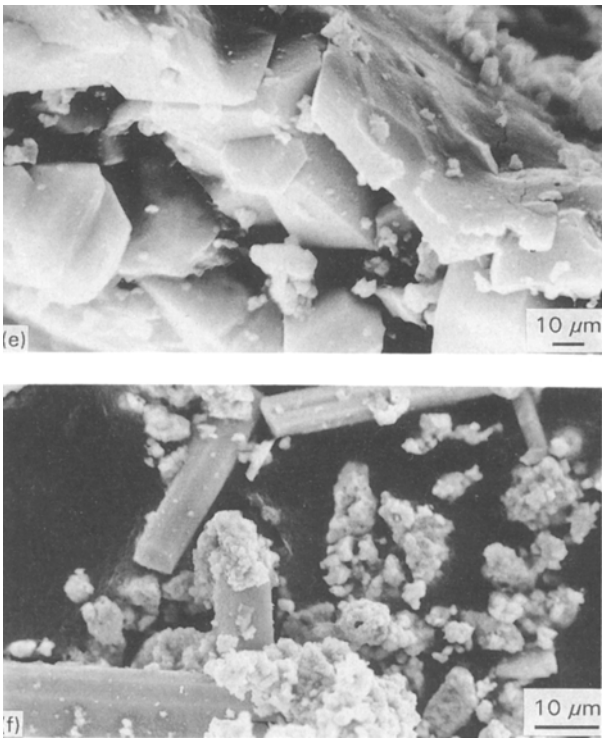

Figure 6 Scanning electron photomicrographs of 29-WPA sample heated at the following temperatures: (a) 60 °C, (b) 130 °C, (c) 350 °C, (d) 600 °C, (e) 750 °C, and (f) 1050 °C.

Fig. 5a, was transformed at about 450 °C to a phase which still retained the basic cubic symmetry of the initial 6-WPA, Fig. 5b and Table V. In spite of a considerable contraction of the unit-cell dimensions, Fig. 3 and Table III, the new phase, which is named the "denuded" Keggin's anion, D-WPA, was stable up to 550 °C, Fig. 5d. Synthesis of this phase at 450 °C was followed on the TGA curve, Fig. 1, by the loss of one water molecule and accordingly the D-WPA formed had the composition $PW_{12}O_{38}$. Extraction of about one molecule of water from the 0-WPA phase between 410 °C and 440 °C was not sufficient to destroy Keggin's framework, which remained stable up to near 550 °C. The D-WPA Keggin's anion phase synthesized in our experiment was stable at room temperature, for a few hours, which does not agree with the results published by Fournier *et al.* in [18]. According to the thermal, XRPD and SEM results, the following reaction scheme can be proposed

$$\text{29-WPA} \xrightarrow{28-31\ ^\circ\text{C}} \text{21-WPA} \xrightarrow{35-42\ ^\circ\text{C}}$$

$$\text{14/6-WPA} \xrightarrow{60\ ^\circ\text{C}} \text{6-WPA} \xrightarrow{175-230\ ^\circ\text{C}}$$

$$\text{0-WPA} \xrightarrow{410-440\ ^\circ\text{C}} \text{D-WPA} \xrightarrow{580-620\ ^\circ\text{C}} \text{bronze}$$

Small disagreements between the temperature intervals given by different methods could be explainable by differences in the experimental conditions and by the particular character of the different methods.

3.2. The structural rearrangements and proton species

To obtain information about modification of the chemical bonds and of the H^+/H_2O ratio in the calcination/dehydration process of the 29-WPA, Raman and i.r. spectroscopic studies were made.

In-situ spectral studies of the phase transformations were made by a Raman microprobe. These investigations were undertaken in order to follow, as a function of quick water elimination, possible changes in the rigid framework, that is, in Keggin's anion. Fig. 7, shows Raman spectra recorded between 100 and 1200 cm^{-1}. Comparing the spectra obtained and the spectra of different phases (6-WPA, 0-WPA and bronze) it is possible to discuss the changes in chemical bonds. Great changes were observed, both in the external and internal modes of the materials at thermally treated 20 °C (29-WPA) and at 100 °C (6-WPA), 250 °C (0-WPA) and 750 °C. The change in the external region is consistent with previous studies which clearly characterize the 29-WPA and 6-WPA phases [6].

It should be pointed out that in the Raman spectra of *n*-WPA, *n*-MoPA and *n*-WSiA, the band intensity of the octahedral modes of WO_6 and MoO_6 is very low with respect to those of the WO_3 or $WO_3 \cdot nH_2O$ type of structures. This probably implies a serious modification of polarizability and thus of the W–O chemical bonds.

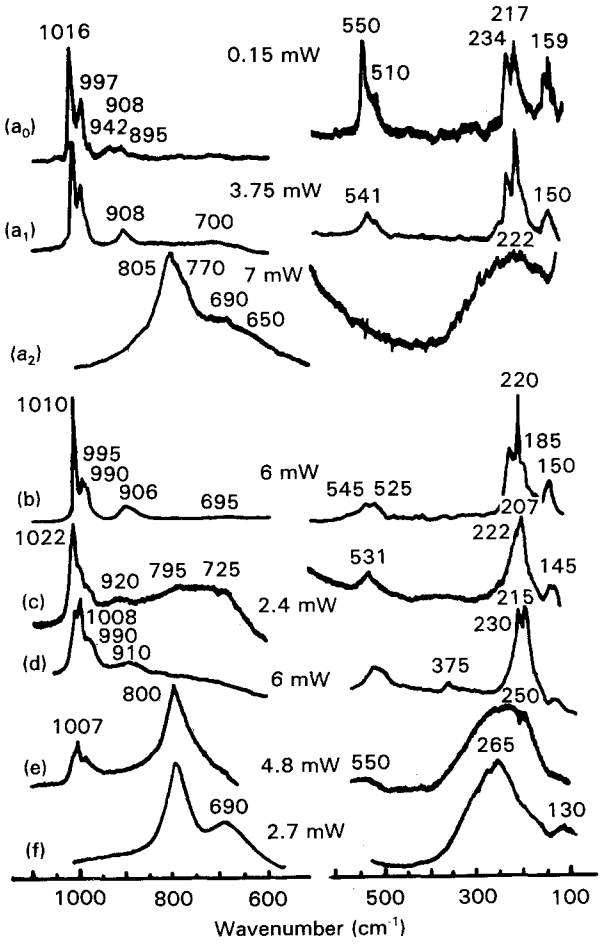

Figure 7 Micro-Raman spectra of the 29-WPA sample heated at different temperatures: (a_0, a_1 a_2) 20 °C (b) 105 °C, (c) 250 °C, (d) 350 °C, (e) 500 °C and (f) 700 °C. Exciting lines 488 nm (a, b, and c) and 514.5 nm (d, e, f) were used at various powers between 0.15 and 7.0 mW.

From the spectroscopic data on the crystal structure and knowledge of $MoPA \cdot 30H_2O$ from [24–25], of $WPA \cdot 21H_2O$ from [21] and of 6-WPA from [20] the following interpretation can be made.

A PO_4 or SiO_4 ion is isolated within a sphere composed of WO_6 or MoO_6 octahedra. There are layers of protonated water between these spheres, and the water loss changes the cubic cell dimension from 2.3328 nm (20 °C) to 1.148 nm (500 °C–the temperature at which the spheres attract each other. In the same temperature interval, Keggin's anions are geometrically stable, but the distance between the oxygen atoms PO_4 and WO_6 decreases from 0.246 nm (29-WPA) to 0.243 nm (6-WPA) [19–21, 24, 25]. The PO_4 or SiO_4 ions thus remain isolated. The other W–O distances are about 0.17 nm (W=O group) in the surface of the sphere or 0.19 nm (W–O–W group).

There are some analogies between the Raman spectra of heteropolyacid hydrates and those of $Zr(HPO_4) \cdot nH_2O$ or HUP (Hydrogen Uranyl Phosphate) [8, 9]. In all cases, heavy ions (Zr, W, Mov) condense with PO_4 ions to form layers. It can thus be asserted that the bands near 1000 cm^{-1} involve mainly PO_4 motions, the bands below 950 cm^{-1} involve W–O with corresponding W–O distances of 0.17 nm; the 700 cm^{-1} bands involve O–W–O mode (mean distance 1.9 nm); and the 400–450 cm^{-1} band involves P–O...W stretching modes (mean distance 0.24 nm). The W–O stretching bands in the spectrum of anhydrous 0-WPA, on the other hand, appear with their expected intensities and their spectrum is similar to that of isopolytungstic acid [26].

In the process of calcination, definite changes are evident in the spectral regions characteristic of proton species. A comparison of the i.r. and Raman spectra of the 29-WPA heated at different temperatures (shown in Figs 7 and 8, and Table IV) shows that in the 6-WPA phase the dioxonium and the oxonium ion exist in dynamic equilibrium [12, 20]. Spectral data point to the destruction of the dioxonium ion $(H_5O_2)_n^+$ [12] in the process of dehydration. This process is accompanied by simultaneous dehydration of the 6-WPA. So the stability of the host lattice of the 0-WPA is due to the presence of trapped protons. These protons can very quickly be reversibly bonded with the water, absorbed during the preparation of the sample for spectra measurement, and build up the $H_3O^+$and $H_5O^+_2$ ions (see Fig. 8, Table IV), that is 6-WPA.

The incoherent inelastic neutron scattering spectra (IINS) confirmed the existence of free protons attached to oxygen atoms of the host lattice in the sample heated at 300 °C [27].

Protons in the 0-WPA are not hydrated and they could be bonded to PO_4 or WO_6. In the first case the situation is the same as in lamellar phosphates, such as $ZrHPO_4 \cdot 1H_2O$, and in the second case the situation is analogous with the tungsten oxide being more or less hydrated.

Daniel *et al.* [28] have studied tungstentrioxide, WO_3, and its hydrates in the octahedra surrounding

TABLE IV Characteristic frequencies (cm^{-1}) of tungstophosphoric heteropolyacid hydrates (*n*-WPA)

29-WPA			6-WPA			0-WPA			PW_8O_6			
Microdil[a]	Raman[b]	i.r.[a]	Microdil[a]	Raman[b1]	i.r.[a]	Microdil[a]	Raman[b2]	i.r.	Microdil[a] 600 °C	Microdil[a] 700 °C	i.r.	Assignment
					1150m, b							$\nu(H_5O_2^+)$
	1077vw	1080s			1080s			1079s				$\nu_3(PO_4)$
1015s	1010s		1010s	1010s		1020s	1020s		1010m, b			$\nu_1(PO_4)$
995m			995m									
		980s	990sh	990m	980s	990m	985sh	985s	990w, b			
940w												$\nu(W=0)$
910vw	925w	918sh	905w	926w		920w	930vw					
895vw	890sh	890s	890sh	890w	890s	900w	895sh	889sh			900m	
		818s, b		800s, b	800w			817s				ν (O–W–O)
							805vw		800s, b	800s,b	791s, b	
			700vw, b			720w			700sh	690m, b		
	687vw										700sh	
		595w			595w		590vw	600sh		670sh		$\nu_4(PO_4)$
550m	538w		545w	536w								
510sh	524w	508m, b	520sh	520w	530w	530w	526w	524w	550w, b			
	476vw			474vw								$\nu_2(PO_4)$
	430vw			430vw								
	412vw			413vw		400vw, b	405vw					
380vw		385s		387vw	390s							ν (W–PO_4)
	370vw				370m		372vw					
	336vw	330m		335vw	330m		338vw					ν (W–PO_4)
320w	312vw			310vw	270w		299vw					
	264vw	255m			250m				290sh	290sh		δ (O–W–O)
	241sh											
235m	223s		235m	232s		220m	222sh		250sb	260s, b		ν (W–O–W)
215m	216s		215s	216s	205w	210s	212s					
	204w	200w			190w							R′PO_4
160m	185w		170sh	157m		180sh	185sh			200sh		
150sh	159w		150w	144m		145m	147w					
							134w			120w		
		120w, b					115vw					
	102s			102s	100w, b		92m					Lattice
	87s			86s			85s					modes
							70vw					
	39vw						47vw					
	24vw			26m								

[a]Not studied below 90 cm^{-1}. (Micro probe Raman spectra)
[b]Spectra recorded in a sealed tube at 300 °C (b1) and at 500 °C (b2).
[c]Temperature of initial thermal treatment.
s, strong; m, medium, w, weak; b, broad; v, very; sh, shoulder

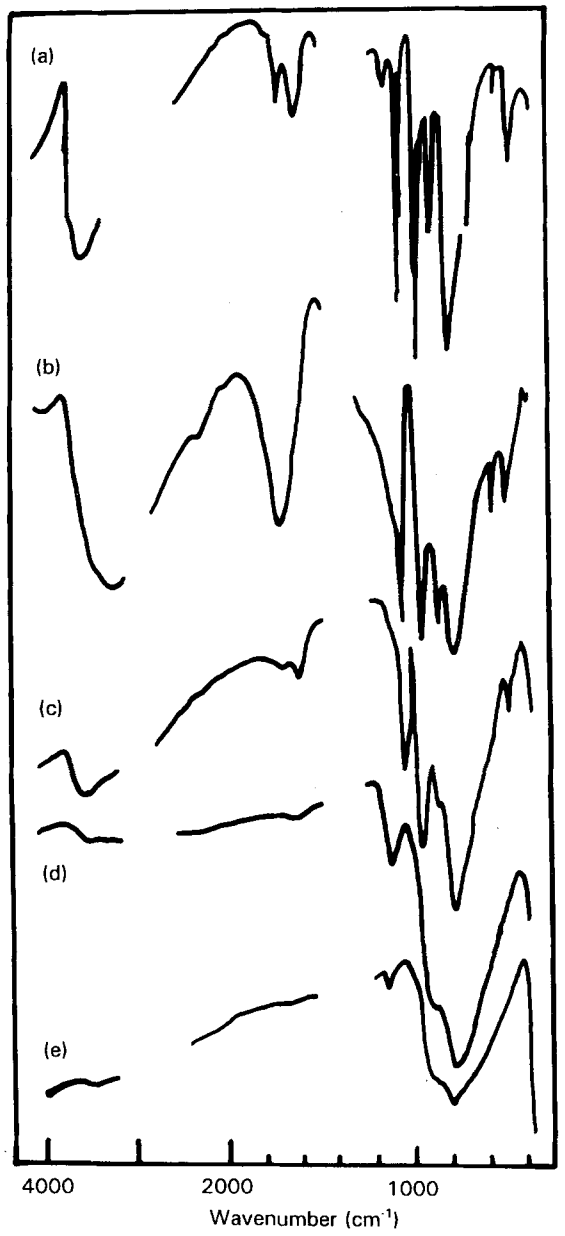

Figure 8 I.r. spectra of the 29-WPA phase heated at the following temperatures: (a) 20 °C, (b) 350 °C, (c) 500 °C (d) 700 °C, and (e) 1000 °C.

W^{6+} (also encountered in WPA-heteropolyacids). The substitution of oxygen atoms by water molecules ($W-OH_2$, $\nu = 370\ cm^{-1}$) resulted in a relatively long bond (0.23 nm), whereas the axially opposite bond is extremely short (0.17 nm), with a character which is similar to a double bond ($W-O$, $\nu = 950\ cm^{-1}$). The same bands are evident in the spectra of the WPA hydrates and the results are consistent with the Cotton curves [29] (Figs. 7 and 8, and Table IV).

The multiplicity of the PO_4 stretching bands (instead of the two ν_1- and ν_3-values for the T_d-symmetry) may be due to symmetry lowering caused by the distortion of the PO_4 ion by the crystal field of W, for instance, and/or due to the existence of non-equivalent PO_4^{-3} ions. The comparison of i.r. and Raman spectra in Figs 7 and 8 does not show mutual exclusion due to symmetry centres but rather it shows the dominant intensity of the PO_4 bands in the Raman spectra and of the WO_6 bands in the i.r. spectra. The modifications appear only for the 6-WPA phase. The question of protonation of PO_4^{3-} ions also arises and the HPO_4^{2-} entity can be present under certain conditions. Such conclusions can find confirmation in the multiplicity of the ν_1 PO_4 band at about $1000\ cm^{-1}$. This band has a shoulder on the lower frequency side in the spectrum of the 6-WPA at room temperature; and, in the spectrum taken at 77 K, the band has a doublet structure (983 and 963 cm^{-1}).

In particular, the formation of HPO_4^{2-} groups in place of PO_4^{3-} can be associated with the formation of W^{5+} ions in the place of W^{6+}. The observed Raman spectra can thus be a (pre) resonance spectrum.

The stretching bands of the PO_4 group are difficult to distinguish in the Raman spectrum of the 0-WPA sample, and then completely disappear in the spectra corresponding to the PW_8O_{26} bronze; see Table IV. This is not surprising, the Raman intensity of W–O bands being usually much larger than that of PO_4, due to a larger polarizability and a higher number of electrons involved in the first kind of the bond.

In the i.r. spectra shown in Fig. 8 the changes become drastic above 600 °C, where the PW_8O_{26} bronze is formed. The destruction of the framework of spherical Keggin's ions at about 600 °C, followed by the formation of the PW_8O_{26} bronze (Figs 5d and 9a) can be explained by a sphere sticking and then opening, leading to the formation of a three-dimensional network of WO_6 octahedra filled with PO_4 tetrahedra – as has been found in numerous crystal structures of tungsten bronze containing phosphorus [30–32]. The corresponding Raman spectra are analogous to those observed for an amorphous WO_3 layer coloured by proton injection, which give rise to strong Raman bands [33]. Three characteristic bands appeared at 800, 690 and 260 cm^{-1}, and they are assignable to O–W–O and W–O–W: the stretching and bending modes respectively (see Table IV).

WPA acids are usually lightly coloured. It is well-known that Keggin's salts can be reduced electrochemically or even photochemically, generally in the presence of an alcohol [34–36]. The electrochemically reduced products with one to four electrons all show absorption triplets near 480–750–1300 nm, 500–660 1100 nm, 570–650–1000 nm and 560–700–1000 nm [37]. These bands have been assigned to the W^{5+}–W^{6+} intervalence transfer between the joined octahedra, as well as to d–d transitions. The electrical compensation is obtained by the fixation of one to

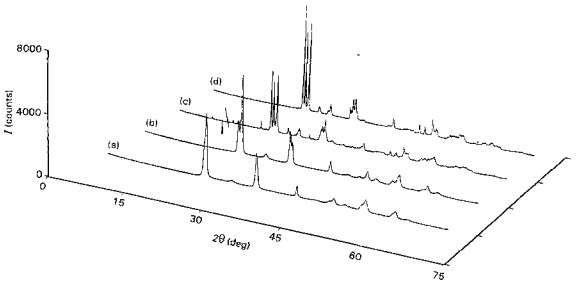

Figure 9 The XRPD traces of PW_8O_{26} bronze polymorphs in the temperature range 650–1150 °C: (a) Cubic, 650 °C, (b) monoclinic, 750 °C, (c) orthorhombic, 1050 °C, and (d) triclinic, 1150 °C.

four protons. The photoreduced product shows a less structured band between 500 and 750 nm, as in the previous case. The beginning of the absorption is situated near 400 nm, which is consistent with the observation of a resonance or preresonance Raman spectrum with the wavelength of the exciting line used in this investigation. The enhancement of the intensity of the bands due to PO_4 ions could indicate that these ions play a particular role during photoreduction and associated protonation.

3.3. Bronze formation and polymorphous transformations

The stability limits of the "denuded" Keggin's framework (D-WPA) phase reaches 500 °C (Fig. 5c), since at 550 °C XRPD patterns show a recrystallization into a new phase, the WO_3 similar compound, (Fig. 5d). This is consistent with the DTA results (exothermal peak at 602 °C). Above this temperature, large noise is present, on the DTA curve (Fig. 1a), which possibly supports the presence of a further transformation, that is, polymorphism of this compound.

The literature data regarding the 29-WPA transformation above 500 °C [38–41] are rather inconclusive about the identification and composition of the phase into which the "denuded" (D-WPA) Keggin's anions phase recrystallizes between 550 °C and 650 °C (Fig. 9a). There is a considerable contribution to this confusion from the polymorphic transition of this phase occurring in further calcination (Fig. 9b–d), as well as its resemblance to the WO_3 polymorphs. According to some authors, thermal treatment of the WPA at 700 °C for 2 h results in a mixture of P_2O_5

TABLE V XRPD data for (a) 0-WPA, (b) D-WPA, (c) PW_8O_{26} (650 °C, cubic) (d) PW_8O_{26} (750 °C, monoclinic), (e) PW_8O_{26} (1050 °C) and (f) PW_8O_{26} (1150 °C), R denotes a rejected line

(a)

I/I_0	H	K	L	D_c (nm)	D_0 (nm)
100	1	1	0	0.85772	0.86047
15	2	0	0	0.60646	0.60731
23	2	1	1	0.49520	0.49469
13	2	2	0	0.42885	0.42908
20	3	1	0	0.38358	0.38444
79	2	2	2	0.35016	0.35031
24	4	0	0	0.30325	0.30285
7	3	3	0	0.28590	0.28586
5	4	2	0	0.27123	0.27122
35	3	3	2R	0.25861	0.25816
14	5	1	0	0.23788	0.23769
4	5	2	1R	0.22146	0.22096
3	6	0	0R	0.20216	0.20188
7	6	1	1	0.19677	0.19664
3	5	4	1R	0.18716	0.18683
14	5	5	0	0.17154	0.17151
10	6	5	1	0.15405	0.15412
4	5	5	4R	0.14930	0.14915
3	6	6	0	0.14295	0.14297

(b)

I/I_0	H	K	L	D_c (nm)	D_0 (nm)
48	1	1	0	0.81268	0.82640
8	2	0	0	0.57465	0.57777
4	2	1	0	0.51398	0.51242
50	2	1	1R	0.46920	0.47735
23	2	2	0R	0.40634	0.41434
100	3	1	0	0.36344	0.36141
40	3	1	1R	0.34653	0.34282
40	3	2	1	0.30716	0.30804
7	4	0	0	0.28732	0.28770
18	3	3	0	0.27089	0.27138
8	4	2	0R	0.25699	0.26060
28	4	2	1R	0.25080	0.25492
7	3	3	2	0.24503	0.24436
15	4	2	2	0.23460	0.23432
17	5	1	0R	0.22539	0.22748
6	5	2	0	0.21342	0.21361
5	5	3	1R	0.19426	0.19612
10	5	3	3	0.17526	0.17558
3	7	1	0	0.16253	0.16211
12	7	2	1	0.15640	0.15626
6	7	3	1	0.14962	0.14951
2	8	1	1	0.14147	0.14177

(c)

I/I_0	H	K	L	D_c (nm)	D_0 (nm)
100	2	0	0	0.37577	0.37666
3	2	1	1R	0.30681	0.31072
56	2	2	0R	0.26571	0.26755
19	2	2	2	0.21695	0.21792
1	3	2	1R	0.20086	0.20307
9	4	0	0	0.18788	0.18760
18	4	2	0	0.16805	0.16831
11	4	2	2	0.15341	0.15364
2	5	1	0R	0.14739	0.14875
3	4	4	0R	0.13285	0.13394
4	6	0	0R	0.12526	0.12579
1	6	2	0	0.11883	0.11871
1	6	2	2	0.11330	0.11330
1	4	4	4R	0.10848	0.10894
1	6	4	0	0.10422	0.10416

(d)

I/I_0	H	K	L	D_c (nm)	D_0 (nm)
41	0	0	2	0.38427	0.38395
100	0	2	0	0.37579	0.37486
1	−1	2	0	0.33435	0.33367
6	−1	1	2	0.31145	0.31080
5	1	1	2	0.30855	0.30833
40	−2	0	2	0.26694	0.26767
26	2	0	2	0.26331	0.26373
14	−2	2	2	0.21762	0.21732
2	2	1	3	0.20098	0.20061
3	0	0	4	0.19214	0.19218
11	−1	0	4	0.18648	0.18657
10	0	1	4	0.18615	0.18611
4	−1	1	4	0.18099	0.18095
6	0	2	4	0.17107	0.17120
	−2	0	4	0.17111	
6	−3	3	1	0.17085	0.17083
10	2	0	4R	0.16919	0.16858
15	−2	1	4	0.16684	0.16685
1	2	3	3	0.16029	0.16033
3	−2	2	4	0.15573	0.15553
9	2	4	2	0.15295	0.15305
3	−1	4	3	0.14861	0.14873

TABLE V Continued

(e)

I/I_0	H	K	L	D_c (nm)	D_0 (nm)
3	1	1	0	1.09407	1.08798
1	0	2	1	0.84216	0.84304
5	1	1	1	0.80623	0.80845
5	1	3	1	0.58199	0.58053
5	2	2	0	0.54703	0.54569
13	2	1	2	0.42169	0.42170
2	2	4	1	0.40273	0.40181
100	3	1	1R	0.38326	0.38464
86	2	5	0	0.37653	0.37621
96	3	3	0	0.36469	0.36532
1	0	3	3	0.35538	0.35555
11	3	1	2	0.33488	0.33496
2	2	5	2	0.31838	0.31819
9	3	3	2	0.31112	0.31165
15	2	3	3	0.30784	0.30843
1	0	0	4	0.29816	0.29830
7	0	2	4	0.28921	0.28902
	4	2	1	0.28929	
1	1	2	4	0.28156	0.28117
	0	6	3	0.28072	
2	1	6	3	0.27371	0.27392
9	4	1	2	0.27188	0.27146
21	3	3	3	0.26874	0.26916
25	2	1	4	0.26669	0.26694
37	3	7	0R	0.26181	0.26242
5	1	9	1	0.25256	0.25260
1	3	7	2	0.23973	0.23930
3	4	5	2	0.23722	0.23757
1	3	3	4	0.23083	0.23042
3	5	1	2	0.22671	0.22683
2	2	10	0	0.22190	0.22179
5	2	10	1	0.21816	0.21780
	1	10	2	0.21747	
12	5	5	1	0.21522	0.21539
1	4	2	4	0.21084	0.21083
3	6	1	0	0.20459	0.20442
3	6	2	0	0.20236	0.20233
3	6	2	1	0.19951	0.19965
2	5	6	2	0.19748	0.19720
8	1	7	5R	0.19283	0.19223
7	0	12	2	0.18810	0.18800
18	3	10	3	0.18279	0.18268
10	6	5	2	0.17977	0.17977
1	7	1	0	0.17554	0.17551
	2	13	0	0.17540	
7	5	8	3	0.17123	0.17123
	5	10	0	0.17114	
6	4	11	2	0.16967	0.16975
7	6	0	4	0.16912	0.16912
	6	8	0	0.16897	
8	6	2	4	0.16744	0.16738
	6	8	1	0.16730	
8	0	13	3	0.16621	0.16610
12	5	9	3	0.16415	0.16415
1	0	15	0	0.15858	0.15843
2	3	14	1	0.15566	0.15571
4	8	0	0	0.15402	0.15398
4	3	12	4	0.15316	0.15318
6	5	11	3	0.15045	0.15054
6	8	4	0	0.14910	0.14902
	6	11	0	0.14891	
3	3	15	1	0.14681	0.14684
1	5	11	4	0.14271	0.14271
1	7	10	1	0.14051	0.14049
	2	16	2	0.14045	
1	1	16	3	0.13837	0.13832

(f)

I/I_0	H	K	L	D_c (nm)	D_0 (nm)
100	0	0	2	0.38416	0.38431
79	0	2	0	0.37610	0.37613
85	2	0	0	0.36542	0.36532
5	−1	2	0	0.33664	0.33664
6	0	−2	1	0.33529	0.33496
4	1	2	0	0.33223	0.33220
4	−1	1	2	0.31456	0.31445
11	1	1	2	0.30916	0.30875
11	0	2	2	0.27133	0.27146
9	−2	0	2R	0.26701	0.26931
20	0	−2	2	0.26623	0.26624
15	−2	2	0	0.26423	0.26422
22	2	0	2	0.26259	0.26242
9	2	2	0	0.25999	0.26005
1	−1	2	2	0.25634	0.25624
2	−2	2	1	0.25184	0.25188
3	1	−2	2	0.25014	0.25022
1	1	1	3	0.22986	0.22974
1	1	3	1	0.22638	0.22633
2	3	1	1	0.22032	0.22032
	−2	2	2	0.22034	
11	−2	−2	2	0.21519	0.21529
	2	−2	2	0.21517	
1	0	3	2	0.21182	0.21182
1	−2	3	0	0.20832	0.20817
	2	0	3	0.20810	
1	−3	2	0	0.20599	0.20592
1	−1	3	2	0.20470	0.20472
2	−1	−3	2	0.19997	0.19994
2	3	−1	2	0.19724	0.19724
8	0	0	4	0.19208	0.19220
7	0	4	0	0.18805	0.18802
15	−1	4	0	0.18283	0.18278
	4	0	0	0.18271	
8	−1	−1	4	0.18011	0.18007
4	3	2	2	0.17919	0.17916
	1	−1	4	0.17907	
2	−1	−3	3	0.17248	0.17252
	1	−3	3	0.17247	
5	−2	0	4	0.17121	0.17121
3	0	4	2	0.17018	0.17026
4	0	−2	4	0.16976	0.16976
4	−3	−3	1	0.16903	0.16909
4	0	−4	2	0.16765	0.16761
7	−4	0	2	0.16608	0.16604
6	2	1	4	0.16509	0.16499
	1	4	2	0.16494	
7	4	0	2R	0.16394	0.16412
5	4	2	0	0.16331	0.16331
1	−2	2	4	0.15728	0.15729
1	−2	4	2	0.15559	0.15559
3	−2	−2	4	0.15440	0.15435
3	−4	2	2	0.15323	0.15322
3	2	−4	2	0.15279	0.15281
4	−4	−2	2	0.15066	0.15067
	4	−2	2	0.15064	
5	−3	4	0	0.15004	0.15004
	0	−1	5	0.15000	
3	−1	−3	4	0.14807	0.14800
	−3	4	1	0.14797	
2	3	1	4R	0.14689	0.14678
	−4	3	1	0.14678	

and WO_3 [42]; according to other authors, the product is a WO_3 oxide alloyed with phosphorus [40].

In our opinion, based on a very careful experimental examination (chemical analysis, XRPD, XRF, i.r. Raman and IINS measurements) the D-WPA Keggin's framework (Fig. 5b–d), after being destroyed at 602 °C, is transformed by solid–solid recrystallization into the PW_8O_{26}-type bronze compound (Figs 5d and 9a and Table V). The IINS measurements show that this compound is free of hydrogen [27].

The bronze formula PW_8O_{26} was calculated from wet chemical analysis-in-weight (P_2O_5 = 3.86%, WO_3= 96.80%; D_{exp} = 7400 kg m^{-3}; D_{cal} = 7501 kg m^{-3}, Z = 1) and the general expression for phosphorus–tungsten bronzes: $(WO_3)_{2m}(PO_2)_4$, where m = 16, for the polymorph synthesized at 600 °C. From our results and knowledge of the field of phosphorus–tungsten bronzes, it could be concluded that PW_8O_{26} compound is a bronze with a very small but regular content of phosphorus. From the structural point of view, this compound belongs to the monophosphate–tungsten–bronze family, whose framework is built as ReO_3-type slabs interconnected through slices of PO_4 tetrahedra. A basic confirmation of such opinion is found in the strong resemblance of the XRPD patterns of cubic WO_3 [41] and to the synthesized PW_8O_{26}. This indirectly suggests a long-range ordering of the PO_4 slices in the crystal lattice. The final proof for the ordering assumption can be obtained from the crystal structure and high-resolution electron microscopy (HREM) investigations.

Another characteristic of the synthesized PW_8O_{26} bronze at 602 °C is a pronounced polymorphism closely resembling the WO_3 compound. It is interesting to note that the PW_8O_{26} bronze synthesized at 602 °C has a cubic symmetry similar to that given in (Fig. 9a and Table III), and it is very similar to the cubic WO_3 [41] obtained by a high-temperature transformation from the A1–WPA salt. An attempt by Siedle *et al.* [41] to synthesize cubic WO_3 from the 29-WPA acid, following the published data of Varfolomeev *et al.* [40], did not succeed. They obtained a tetragonal WO_3, which in our examination appeared as a second PW_8O_{26} polymorph, Fig. 9b. The correct symmetry of the pronounced polymorphism of PW_8O_{26} obtained at 750 °C in our experiment is monoclinic; this does not agree with previous findings [40, 41]. This phase is stable up to 850 °C (Fig. 9b, Table V).

The SEM investigation of the PW_8O_{26} polymorphs at 600 °C and 750 °C revealed the morphologies of both the polymorphs. The bronze polymorph at 600 °C showed the presence of tabular single crystals with a length of a few micrometres and a thickness of about 0.5 μm, opposite the cubic habitus of the 0-WPA crystals at 350 °C. The crystals of monoclinic PW_8O_{26} polymorph, at 750 °C, have a habit corresponding to the lower crystal symmetry (Fig. 6e), where most of the crystals have a tabular habit with well-developed forms.

Further thermal treatment of the monoclinic phase above 850 °C produced transformation to a new phase (a third polymorph) at 950 °C. This phase was stable up to 1050 °C (Fig. 9c, and Tables III and V). Our attempts to identify the PW_8O_{26} phase at 1050 °C in the JCPDS file did not succeed. The suggestion of exolution [42] of $2WO_3 \cdot P_2O_5$ or some other mixed phosphorus–tungsten oxide also could not be confirmed either by XRPD or spectral data. It is important to state that the PW_8O_{26}-bronze phase (third polymorph, Fig. 9c) had no analogue among the WO_3 polymorphs [43–47]. The SEM investigations of the third PW_8O_{26} polymorph revealed elongated prismatic habits of crystals, Fig. 6f, which is consistent with the XRPD measurements.

Prolonged annealing of the third bronze polymorph at 1150 °C produced a new polymorphic transformation in the triclinic PW_8O_{26} bronze phase (Fig. 9d, and Tables III and V), which had an analogue among the WO_3 phases [45].

According to previous results, the following polymorphous transformation scheme, may be proposed for the PW_8O_{26}-type monophosphate bronze:

$$\xrightarrow[\text{cubic}]{600-700\,^\circ C} \xrightarrow[\text{monoclinic}]{750-850\,^\circ C} \xrightarrow[\text{orthorhombic}]{950-1050\,^\circ C} \xrightarrow[\text{triclinic}]{1150\,^\circ C}$$

It has to be noted that the process of the phosphorus–bronze formation from heteropolyacids is very quick and elegant in relation to the other known methods.

4. Conclusion

Structural transformation of the rigid framework and its containing protonic species of the 29-WPA heteropolyacid were studied using the same sample in all the experiments in the process of calcination/dehydration. A correlation between thermal (DTA, TGA and DSC), XRPD and SEM data, as well as the spectral data, was undertaken with the aim of obtaining a global picture of the structural transformation and protonic-species equilibrium in WPA hydrates from room temperature up to 1150 °C.

All the phases found in the process of calcination/dehydration of the 29-WPA sample were discussed from the point of view of the structure, the stability, and the nature of chemical bonds.

It was found that there was some similarity between n-WPA and $WO_3 \cdot nH_2O$ hydrates. The possibility of the substitution of one oxygen of WO_6 octahedra by H_2O resulted in the appearance of W–OH_2 oscillators with a rather long bond 0.23 nm. The opposite axial bond was short (0.17 nm) giving this terminal bond a double-bond character (W=O). The existence of non-equivalent PO_4 tetrahedra was also evident from the i.r. and Raman spectra.

It is evident that the dehydration process modified the protonic species equilibrium and the crystal symmetry. Although the process of dehydration affected the lattice parameters (a_0 and V_0), and modified the molecular bonds, the structure of the Keggin's ion framework was not destroyed up to 580 °C.

Phosphorus-containing bronze, PW_8O_{26} is a new material synthesized from Keggin's anion framework

as a precursor by solid–solid recrystallization. In the temperature range from 620–1150 °C, synthesized cubic bronze undergoes three polymorphous transitions up to 1150 °C. Phosphorous–bronze polymorphs in this paper were described for the first time; and some of these are new (orthorhombic at 1050 °C) without analogues in WO_3 compounds.

Acknowledgements

This paper was supported in part by the Serbian Research Fund. We would like to thank Mrs L. Mihovilovic for chemical analysis. The authors are grateful to Dr A. Novak for useful comments and suggestions, and to Dr B. Forsyth for reading and making useful comments on the manuscript.

References

1. O. NAKAMURA, T. KODAMA, J. OGINO and Y. MIYAKE *Chem. Lett.*, (1979) 17.
2. O. NAKAMURA, I. OGINO and T. KODAMA, *Solid State Ionics* **3/4** (1981) 347.
3. S. K. MOHAPATRA, G. D. BOYD, F. G. STORZ, S. WAGNER and F. WUDL, *J. Electrochem. Soc.* **126** (1979) 805.
4. R. C. T. SLADE, H. A. PRESSMAN and E. SKOU, *Solid State Ionics* **38** (1990) 207.
5. R. C. T. SLADE, I. M. THOMSON, R. C. WARD and C. POINSIGNON, *J. Chem. Soc., Chem. Commun.* (1987) 726.
6. G. J. KEARLEY, R. P. WHITE, C, FORANO and R. C. T. SLADE, *Spectrochim. Acta A* **46** (1990) 419.
7. PH. COLOMBAN, C. DOREMIEUX-MORIN, Y. PIFFARD, M. H. LIMAGE and A. NOVAK, *J. Mol. Struct.* **213** (1989) 83.
8. PH. COLOMBAN and A. NOVAK, *ibid.* **198** (1989) 277.
9. M. PHAM-THI and PH. COLOMBAN, *J. Less-Commun. Metal.* **108** (1985) 747.
10. *Idem. J. Mater. Sci.* **21** (1986) 1591.
11. U. MIOČ, PH. COLOMBAN and A. NOVAK, *J. Mol. Struct.* **218** (1990) 123.
12. U. MIOČ, M. DAVIDOVIĆ, N. TJAPKIN, PH. COLOMBAN and A. NOVAK, *Solid State Ionics* **46** (1991) 103.
13. P. E. WERNER, *Z. Kristall*, **120** (1964) 375.
14. J. W. VISSER, *J. Appl. Cryst.* **2** (1969) 89.
15. R. GARVEY, Least Squares Unit Cell Refinement, Version 86.2., Department of Chemistry, North Dakota State University, 1987.
16. D. E. APPLEMAN and H. T. EVANS Jr., U. S. Department of Commerce National Technical Information Service. **216** (1973) 188.
17. U. B. MIOČ, to be published.
18. M. FOURNIER, CH. FEUMI-JANTOU, CH. RABIA, G. HERVE' and S. LAUNAY, *J. Mater. Chem.* **2** (1992) 971.
19. N. R. NOE-SPIRLET, G. N. BROWN, W. R. BUSING and H. A. LEVY, *Acta Cryst A* **31** (1975) 580.
20. G. M. BROWN, M. R. NOE-SPIRLET, W. R. BUSING and H. A. LEVY., *ibid. B* **33** (1977) 1038.
21. M. R. NOE-SPIRLET and W. R. BUSING, *ibid. B* **34** (1978) 907.
22. H. D'AMOUR and R. ALLMANN, *Z. Kristall.* **143** (1976) 1.
23. R. ALLMANN and H. D'AMOUR, *ibid.* **141** (1975) 161.
24. C. J. CLARK and D. HALL, *Acta Cryst.* **B32** (1976) 1545.
25. R. STANDBERG, *Acta Chem. Scand. A* **29** (1975) 359.
26. H. OKAMOTO, K. YAMANAKA and T. KUDO, *Mater. Res. Bull.* **21** (1986) 551.
27. U. MIOČ, M. DAVIDOVIC', J. TOMKINSON and N. TJAPKIN, Annual Report, ISIS, Vol. II, Rutherford Appleton Laboratory, Didcot, UK, p. 331; and V. MIOČ, PH. COLOMBAN, M. DAVIDOVIČ and J. TOMKINSON, *J. Mol. Struct.* (submitted).
28. M. F. DANIEL, B. DESBAT, J. C. LASSEGUES, B. GERAND and M. FIGLARZ, *J. Solid State Chem.* **67** (1987) 235.
29. F. A. COTTON and R. M. WING, *Inorg. Chem.* **4** (1965) 867.
30. A. BENMOUSSA, PH. LABBE, D. GROULT and B. RAVEAU, *J. Solid State Chem.* **44** (1982) 318.
31. PH. LABBE, M. GOREAUD and B. RAVEAU, *ibid.* **61** (1986) 324.
32. S. L. WANG, C. C. WANG and K. H. LII, *ibid.* **82** (1989) 298.
33. M. PHAM-THI and G. VELASCO, *Solid State Ionics* **14** (1984) 217.
34. P. KERSERHO, Thesis, University of Paris (1982).
35. E. PAPACONSTANTINOU, D. DIMITIKALI and A. POLITOU, *Inorg. Chem. Acta* **46** (1980) 155.
36. E. PAPACONSTATINOU, *J. Chem. Soc., Chem. Commun.* (1982) 12.
37. G. M. VARGA, E. PAPACONSTATINOU and M. T. POPE, *Inorg. Chem.* **9** (1970) 662.
38. H. HAYASHI and J. B. MOFFAT, *J. Catal.* **77** (1982) 473.
39. *Idem., ibid.* **83** (1983) 192.
40. M. B. VARFOLOMEEV, V. V. BURLEAEV, T. A. TOPORENSKAYA, H. J. LUNK, W. WILDE und W. HILMER, *Z. Anorg. Allg. Chem.* **472** (1981) 185.
41. A. R. SIEDLE, T. E. WOOD, M. L. BROSTROM, D. C. KOSKENMAKI, B. MONTEZ and E. OLDFIELD., *J. Amer. Chem. Soc.* **111** (1989) 1665.
42. H. J. LUNK, M. B. VARFOLOMEEV and W. HILMER, *Zh. Neorg. Khim.*, **28** (1983) 936.
43. E. SALJE and K. VISWANATHAN, *Acta Cryst. A* **31** (1975) 356.
44. E. SALJE, *ibid. B* **33** (1977) 574.
45. R. DIEHL, G. BRANDT and E. SALJE, *Acta Cryst. B* **34** (1978) 1105.
46. W. L. KEHL, R. G. HAY and D. WAHL, *J. Appl. Phys.* **23** (1952) 212.
47. B. GERAND, G. NOWOGROCKI, J. GUENOT and M. FIGLARZ, *J. Solid State Chem.* **29** (1979) 429.

Received 29 July
and accepted 21 December 1993